

Vlasov simulations of collisionless self-gravitating systems and astrophysical plasmas

Kohji Yoshikawa

Division of Astrophysics

Center for Computational Sciences, University of Tsukuba

CCS-EPCC Workshop

December 7 - 8, 2017, CCS, Univ. of Tsukuba

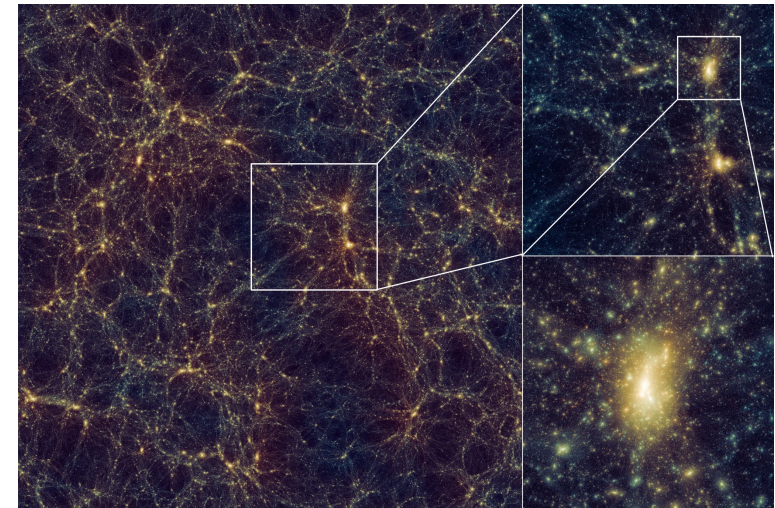
collaborators: Satoshi Tanaka (CCS, Univ. of Tsukuba)
Takashi Minoshima (JAMSTEC)
Naoki Yoshida (Univ. of Tokyo)

N-body Simulation of Self-Gravitating Systems

- ▶ a standard method for simulations of **self-gravitating systems** (galaxies, clusters of galaxies, the large-scale structure in the universe) for more than 40 years.
- ▶ the mass distribution is sampled by particles in the 6D phase-space volume (\mathbf{x} , \mathbf{p}) in a Monte-Carlo manner.

$$\frac{d\mathbf{v}_i}{dt} = \sum_j \frac{m_j(\mathbf{r}_j - \mathbf{r}_i)}{|\mathbf{r}_j - \mathbf{r}_i|^3}$$

- ▶ sophisticated algorithms to treat large number of particles such as **Tree and TreePM methods** developed



Ishiyama 2013

Particle-In-Cell (PIC) Simulation of Plasmas

- ▶ Particle-based approach to solve collisionless (astrophysical) plasma

$$\frac{d\mathbf{v}_i}{dt} = \frac{q_i}{m_i} \left(\mathbf{E} + \frac{\mathbf{v}_i \times \mathbf{B}}{c} \right)$$

- ▶ E - and B -fields are computed in the finite difference manner

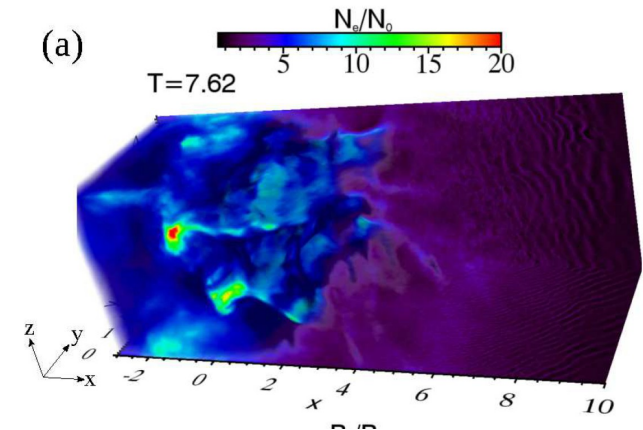
$$\mathbf{x}_i, \mathbf{v}_i \longrightarrow \mathbf{J}$$

$$\frac{\partial \mathbf{E}}{\partial t} = c \nabla \times \mathbf{B} - 4\pi \mathbf{J}$$

$$\frac{\partial \mathbf{B}}{\partial t} = -c \nabla \times \mathbf{E}$$

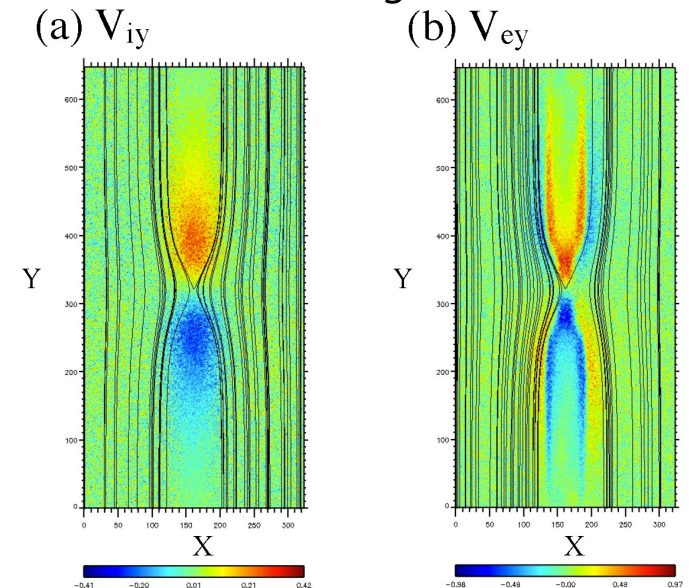
- ▶ particle acceleration in collisionless shock
- ▶ magnetic reconnection

3D PIC simulation of collisionless shock



Matsumoto et al. (2017)

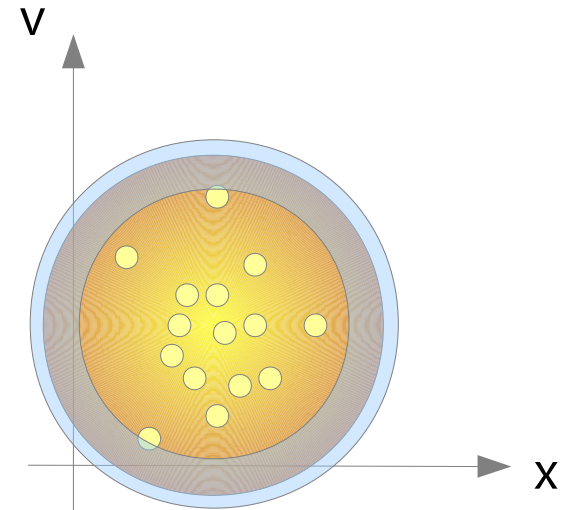
PIC simulation of magnetic reconnection



(pCANS web page)

Drawbacks of Particle Simulations

- ▶ intrinsic contamination of **shot noise** in physical quantities
- ▶ not good at simulating kinetic physical processes in which the tail of the distribution function plays important roles
 - matter in the tail is not fairly sampled in particle simulations
 - collisionless damping, two-stream instability
 - magneto-rotational instability starting from high-beta plasmas
- ▶ The grid spacing of PIC simulations should be less than the Debye length.
 - difficult to simulate phenomena in the macroscopic scale



Vlasov Simulations

- ▶ Simulate self-gravitating systems and plasmas by directly solving the Vlasov equation in a finite volume manner

$$\frac{\partial f}{\partial t} + \frac{d\mathbf{x}}{dt} \cdot \frac{\partial f}{\partial \mathbf{x}} + \frac{d\mathbf{p}}{dt} \cdot \frac{\partial f}{\partial \mathbf{p}} = 0$$

$f(\mathbf{x}, \mathbf{p}, t)$: distribution function in six-dimensional phase space

▶ Vlasov-Poisson simulation

- self-gravitating system
- electro-static plasma

$$\frac{\partial f}{\partial t} + \mathbf{v} \cdot \frac{\partial f}{\partial \mathbf{x}} - \nabla \phi \cdot \frac{\partial f}{\partial \mathbf{v}} = 0$$

$$\nabla^2 \phi = 4\pi G \rho = 4\pi G \int f d^3 \mathbf{v}$$

▶ Vlasov-Maxwell simulation

- magnetized plasma

$$\frac{\partial f_s}{\partial t} + \mathbf{v} \cdot \frac{\partial f_s}{\partial \mathbf{x}} + \frac{q_s}{m_s} \left(\mathbf{E} + \frac{\mathbf{v} \times \mathbf{B}}{c} \right) \cdot \frac{\partial f_s}{\partial \mathbf{v}} = 0$$

$$\frac{\partial \mathbf{E}}{\partial t} = c \nabla \times \mathbf{B} - 4\pi \mathbf{J}$$

$$\frac{\partial \mathbf{B}}{\partial t} = -c \nabla \times \mathbf{E}$$

$$\mathbf{J} = \sum_s \int q_s \mathbf{v} f_s d^3 \mathbf{v}$$

Vlasov Simulations

- ▶ Free from shot noise contamination
- ▶ Good at capturing kinematic physical processes
 - collisionless damping, dynamical friction etc in self-gravitating systems
 - Landau damping, weibel instability etc in astrophysical plasma
- ▶ Free from mesh size constraint to the Debye length
- ▶ requires huge amount of memory and computational costs
had not been practical for a long time
- ▶ solves hyperbolic PDE instead of ODE in particle simulations
 - ➡ inevitable numerical diffusion
 - ➡ need for sophisticated less diffusive numerical schemes

Vlasov-Poisson Simulation in 6D phase space

Yoshikawa, Yoshida, Umemura (2013)

► directional splitting method

$$\frac{\partial f}{\partial t} + \vec{v} \cdot \frac{\partial f}{\partial \vec{x}} - \nabla \phi \cdot \frac{\partial f}{\partial \vec{v}} = 0 \quad \longrightarrow \quad \left\{ \begin{array}{l} \frac{\partial f}{\partial t} + v_i \frac{\partial f}{\partial x_i} = 0 \quad (i = 1, 2, 3) \\ \frac{\partial f}{\partial t} - \frac{\partial \phi}{\partial x_i} \frac{\partial f}{\partial v_i} = 0 \quad (i = 1, 2, 3) \end{array} \right.$$

$$f(\vec{x}, \vec{v}, t^{n+1}) = T_{v_x}(\Delta t/2) T_{v_y}(\Delta t/2) T_{v_z}(\Delta t/2)$$

$$T_x(\Delta t) T_y(\Delta t) T_z(\Delta t)$$

$$T_{v_x}(\Delta t/2) T_{v_y}(\Delta t/2) T_{v_z}(\Delta t/2) f(\vec{x}, \vec{v}, t^n)$$

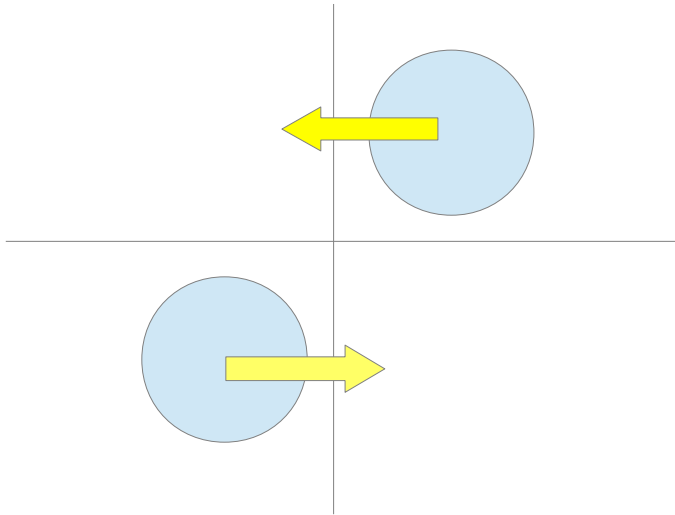
$T_\ell(\Delta t)$: advection along ℓ -direction

► numerical scheme for a one-dimensional advection equation

Positive and Flux Conservative (PFC) scheme

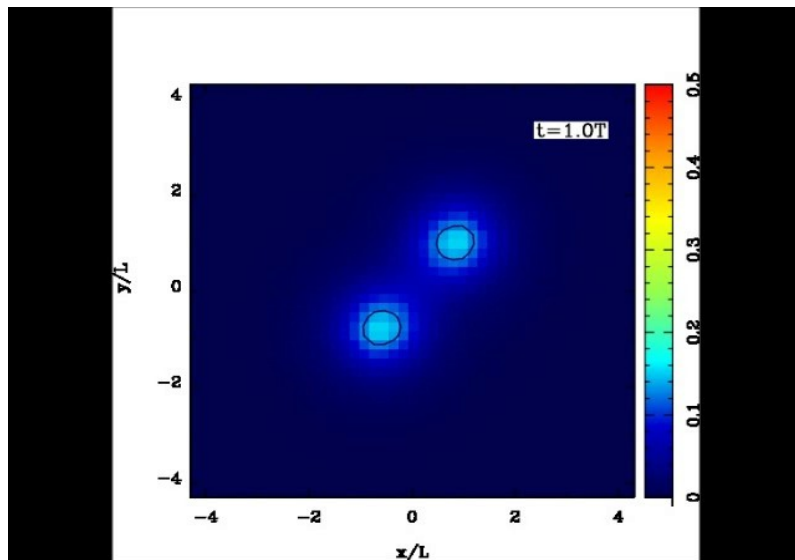
Filbet, Sonnendrücker, Bertrand (2001)

Merging of Two Spheres

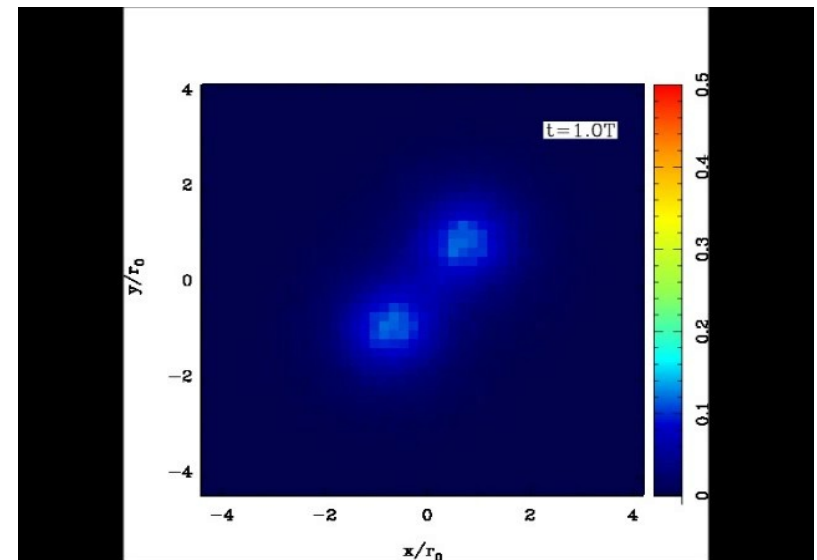


- ▶ offset merging of two king self-gravitating spheres
- ▶ comparison with a equivalent N-body simulations, in which each King sphere is represented with a million particles

Vlasov simulation



N-body simulation



Grav. Instablity and Collisionless Damping

Initial condition

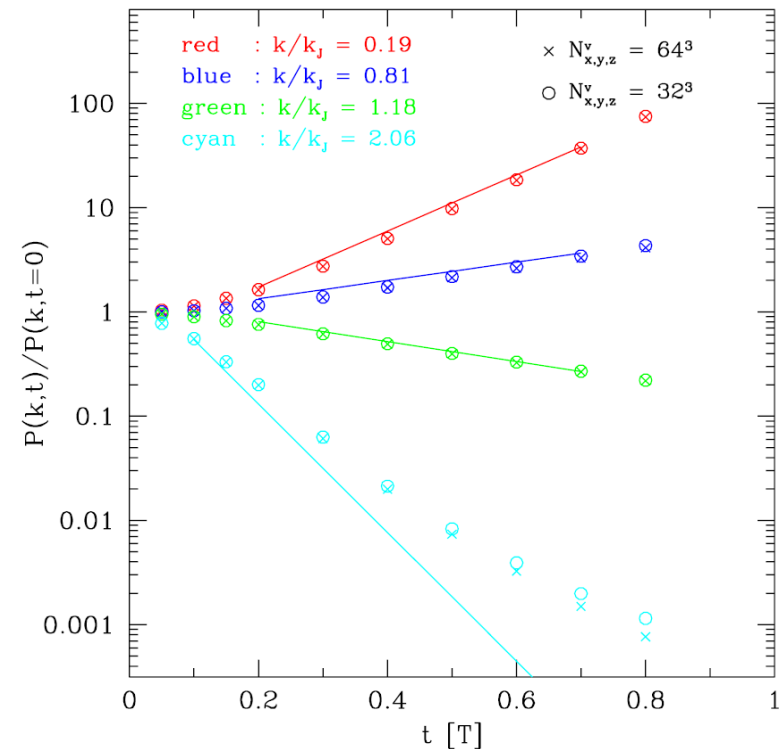
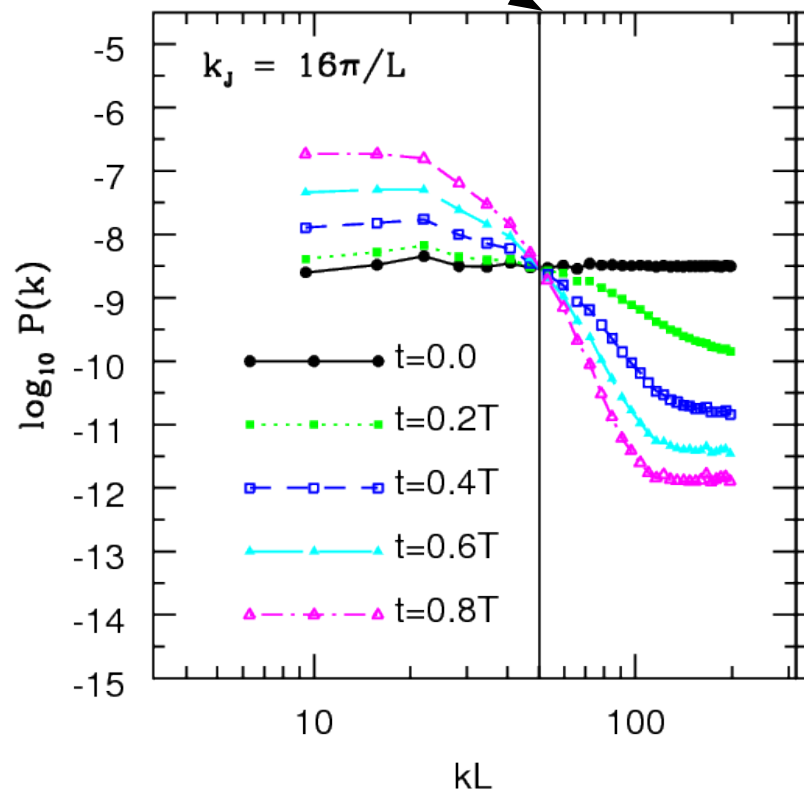
$$\left\{ \begin{array}{l} f(\vec{x}, \vec{v}, t = 0) = \frac{\bar{\rho}(1 + \delta(\vec{x}))}{(2\pi\sigma^2)^{3/2}} \exp\left(-\frac{|\vec{v}|^2}{2\sigma^2}\right) \\ \rho(x, t = 0) = \bar{\rho}(1 + \delta(x)) \end{array} \right.$$

$k < k_J$: gravitational instability

$k > k_J$: collisionless damping

- The initial density fluctuation $\delta(x)$ is given so that it has a **white noise** power spectrum.

$$k = k_J$$



lines : theoretical prediction

New High-Order Schemes for Vlasov Simulation

Higher-Order Advection Schemes

► curse of dimensionality in Vlasov simulations

huge memory consumption due to high dimensionality of phase space

➡ size of numerical simulation is limited by the amount of available memory

► how to overcome

- adaptive mesh refinement

- higher-order schemes for the advection equation

$$\frac{\partial f(x, t)}{\partial t} + c \frac{\partial f(x, t)}{\partial x} = 0$$

► mathematical and physical requirements

- monotonicity

monotonicity-preserving (MP) constraints (Suresh & Huynh 1997)

- positivity

a new positivity-preserving (PP) limiter in the form of a flux limiter

► spatially fifth- and seventh-order schemes with monotonicity- and positivity-preserving features.

(c.f. The PFC scheme has a spatially third-order accuracy.)

Naming Convention of the Schemes

XX-MPP5

RK : 3-stage temporary 3rd order Runge-Kutta time integration

SL : single-stage semi-Lagrangian time integration

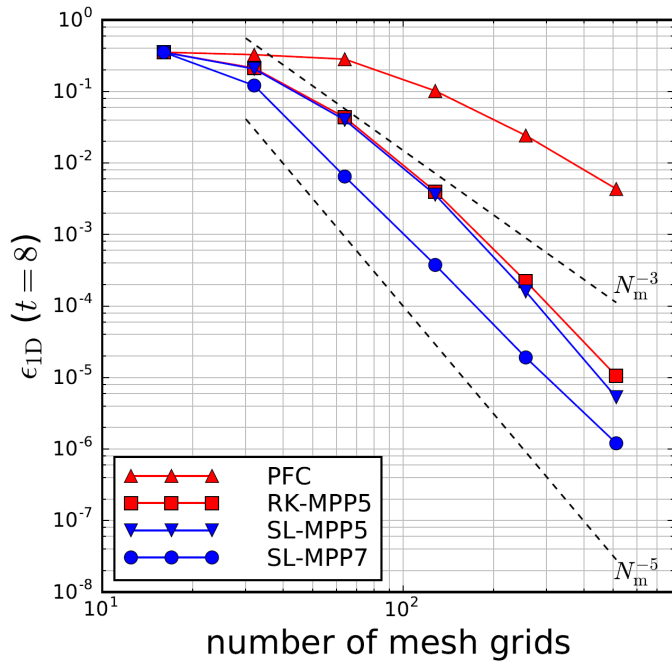
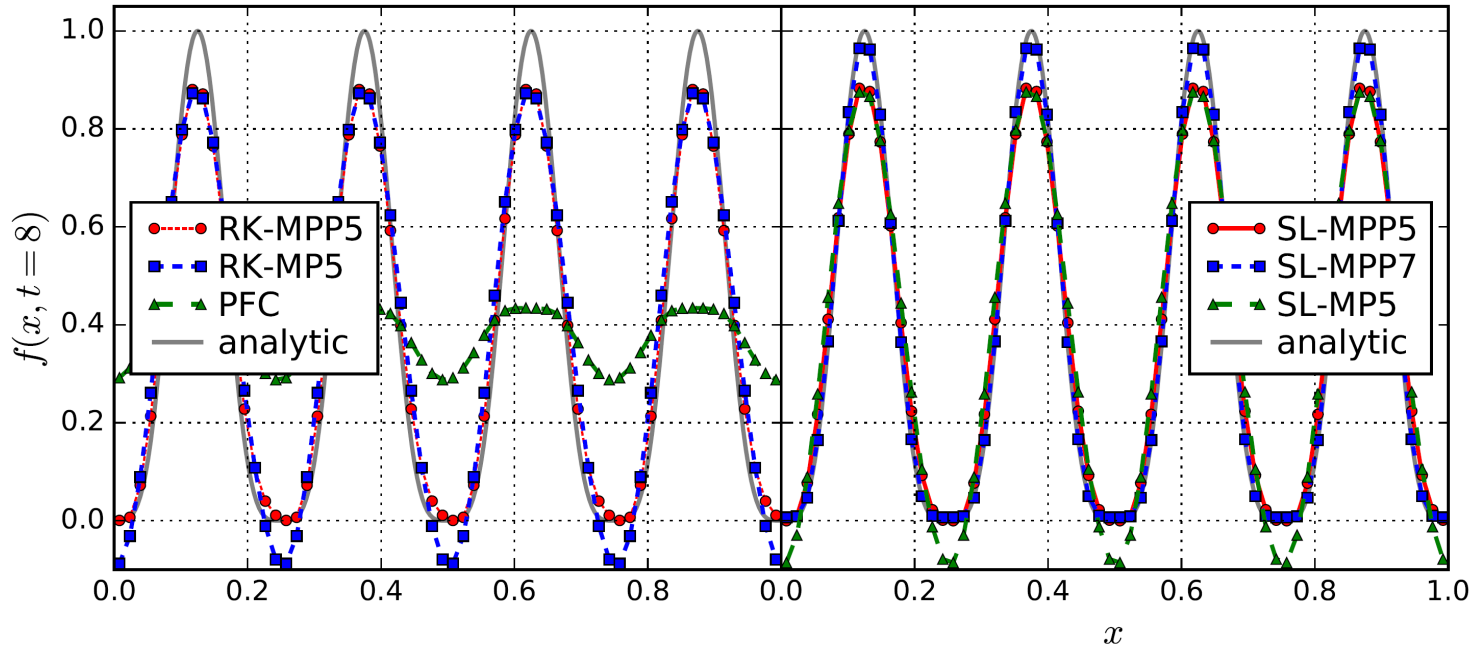
MPP : monotonicity and positivity preserving

MP : monotonicity preserving

final digit : the spatial order of accuracy

Linear Advection

► linear advection of $f(x, t = 0) = \sin^4(4\pi x)$



- ▶ The result of PFC scheme is severely smeared.
- ▶ Schemes w/o PP limiter yield significant negative value around the minima.
- ▶ Only 7th-order scheme (SL-MPP7) can reproduce the maxima.

1D Self-Gravitating System

► one-dimensional space with periodic boundary condition

► initial condition

$$f(x, v, t = 0) = \frac{\bar{\rho}[1 + A \cos(kx)]}{(2\pi\sigma^2)^{1/2}} \exp\left(-\frac{v^2}{2\sigma^2}\right)$$

$$\rho(x, t = 0) = \bar{\rho}[1 + A \cos(kx)]$$

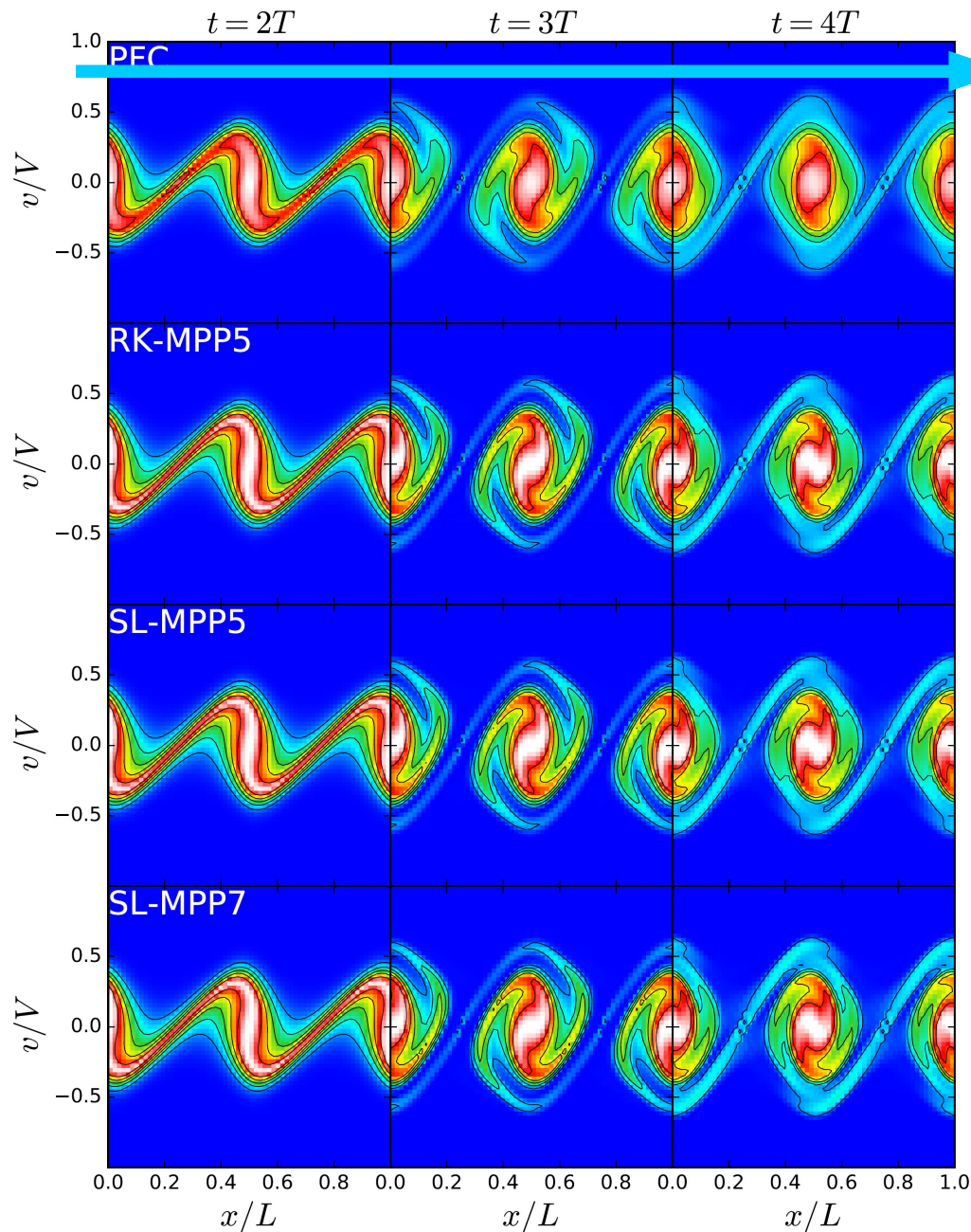
► critical Jeans wave number

$$k_J = \left(\frac{4\pi G \bar{\rho}}{\sigma^2}\right)^{1/2}$$

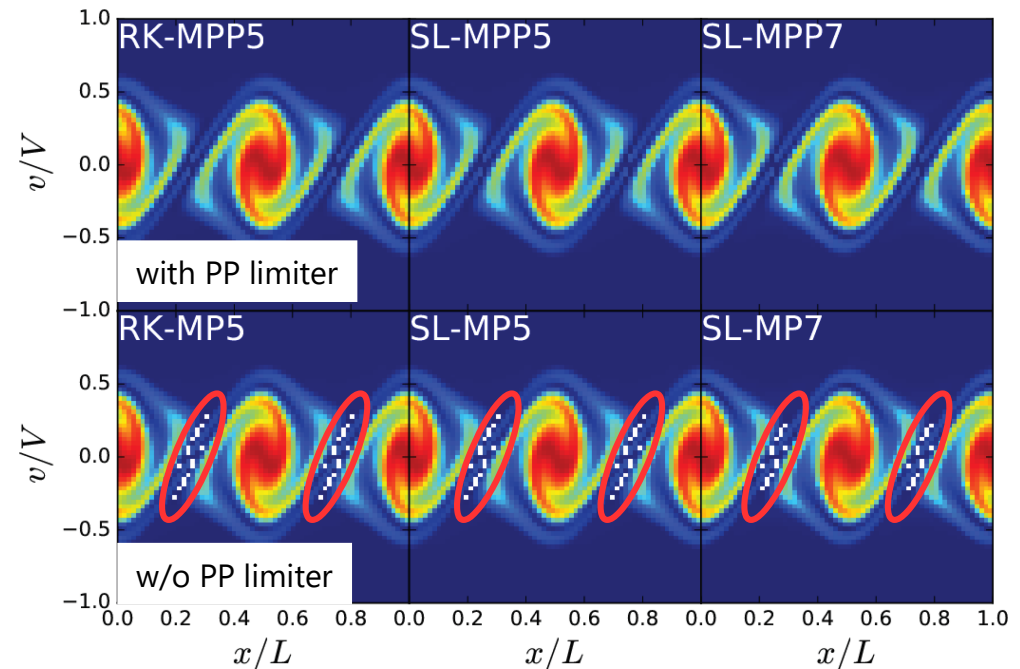
$$\left\{ \begin{array}{ll} k < k_J & \longrightarrow \text{gravitational instability} \\ k > k_J & \longrightarrow \text{collisionless damping} \end{array} \right.$$

1D Self-Gravitating System

$$k/k_J = 0.5 \quad A = 0.01 \quad N_x = N_v = 64$$



As time proceeds, numerical diffusion takes place and smear small structures in the lower-order schemes.



Negative regions in the lower panels disappear in the results with positivity preserving limiter.

Application To Cosmological Neutrinos

Cosmological Relic Neutrinos

▶ massive neutrinos in the universe

- lots of neutrinos in our universe decoupled at early stage of the universe when they are relativistic.
- Discovery of neutrino oscillation
$$\sum m_\nu > 0.05 \text{ eV}$$
- currently non-relativistic and gravitationally interacting with cold dark matter (CDM)
- absolute mass of neutrinos and its hierarchy are still unknown

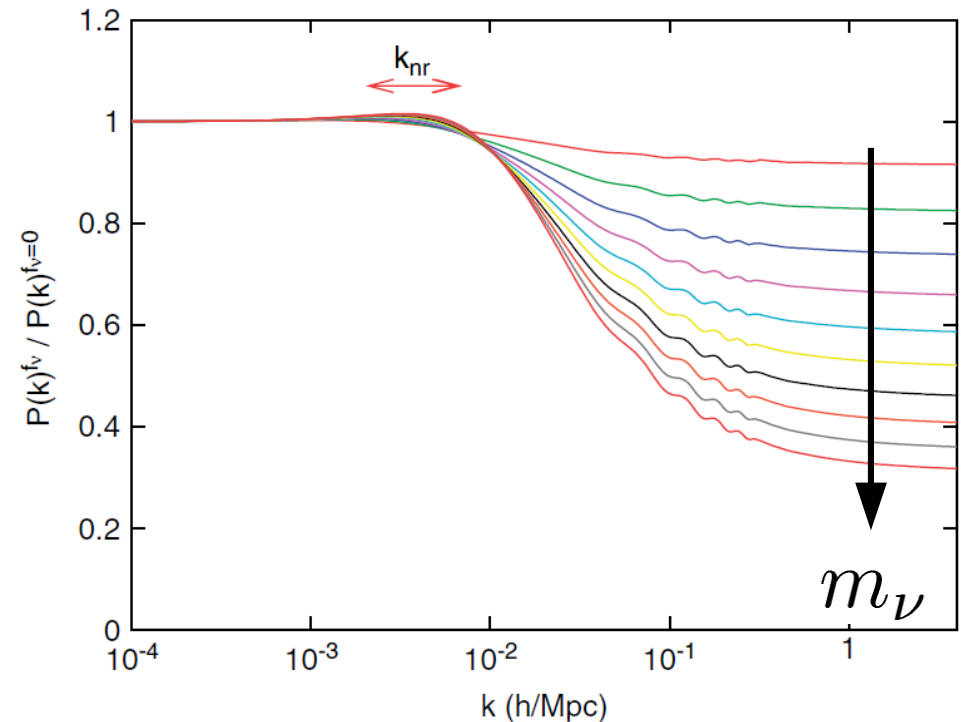
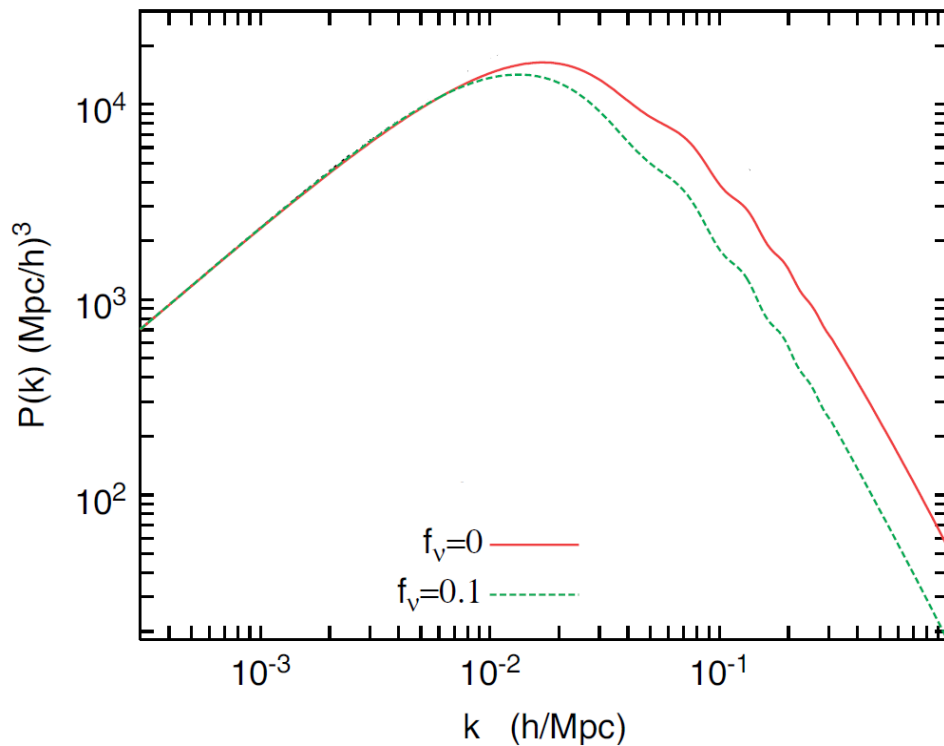
▶ dynamical effect of massive neutrinos

free streaming (collisionless damping)

- large velocity dispersion of neutrinos $\sigma \sim 150(1+z) \left(\frac{m_\nu}{1\text{eV}}\right)^{-1} \text{ km/s}$
- growth of density fluctuation suppressed beyond the damping scale

$$k_{\text{FS}} = \left(\frac{4\pi G\rho}{\sigma^2}\right)^{1/2} \Rightarrow \lambda_{\text{FS}} \sim 640 \left(\frac{\Omega_{\text{m}}}{0.3}\right)^{-1/2} \left(\frac{m_\nu}{1\text{eV}}\right)^{-1/2} h^{-1} \text{Mpc}$$

Collisionless Damping on LSS



- density fluctuation suppressed at scales smaller than the damping scale.
- the amount of suppression depends on the mass of neutrinos
- the mass (and its hierarchy) of neutrinos can be estimated with such damping feature.
- non-linear features should be investigated with numerical simulations.

Initial Condition

► cosmological parameters

PLANCK 2015 results : $\Omega_{\text{m}} = 0.308$, $\Omega_{\Lambda} = 0.692$, $\Omega_{\text{b}} = 0.0484$, $h = 0.678$

curvature fluctuation : $A_{\text{s}} = 2.3723 \times 10^{-9}$ (pivot scale : $k = 0.002 \text{ Mpc}^{-1}$)

► total neutrino mass

$$\sum_i m_i = 0.4 \text{ eV} \quad (\Omega_{\nu} = 0.0043 h^{-2})$$

► initial condition created at redshift of $z_{\text{i}} = 10$

► computaional domain: $L_{\text{box}} = 20000 h^{-1} \text{ Mpc}, 2000 h^{-1} \text{ Mpc}, 200 h^{-1} \text{ Mpc}$

► number of particles / number of mesh grids

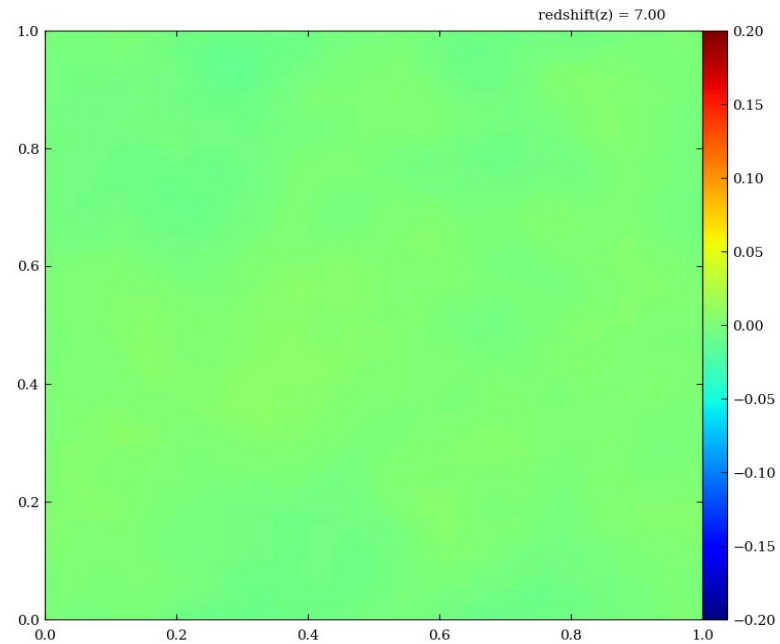
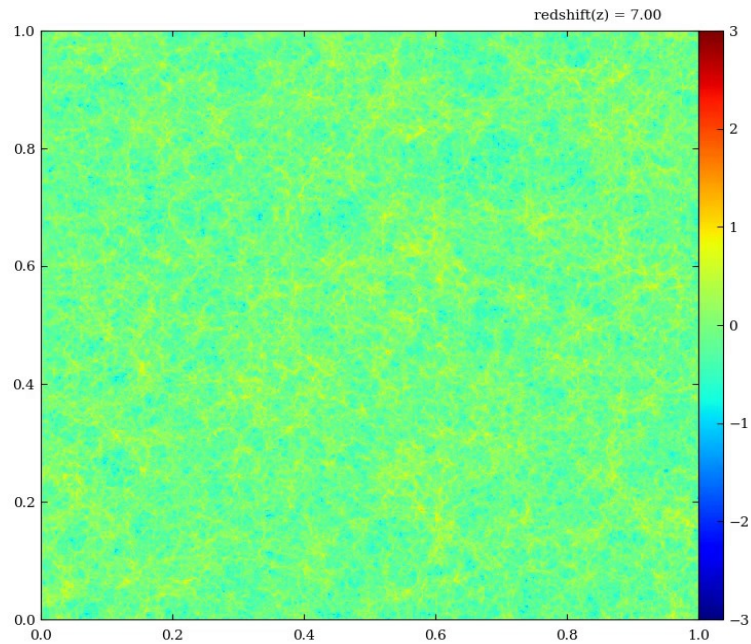
N-body simulation : $N_{\text{p}} = 1024^3$

Vlasov simulation : $N_{\text{x}} = 128^3, N_{\text{v}} = 32^3$

CDM and neutrino distribution

CDM

neutrino



$\log_{10}(1 + \delta)$



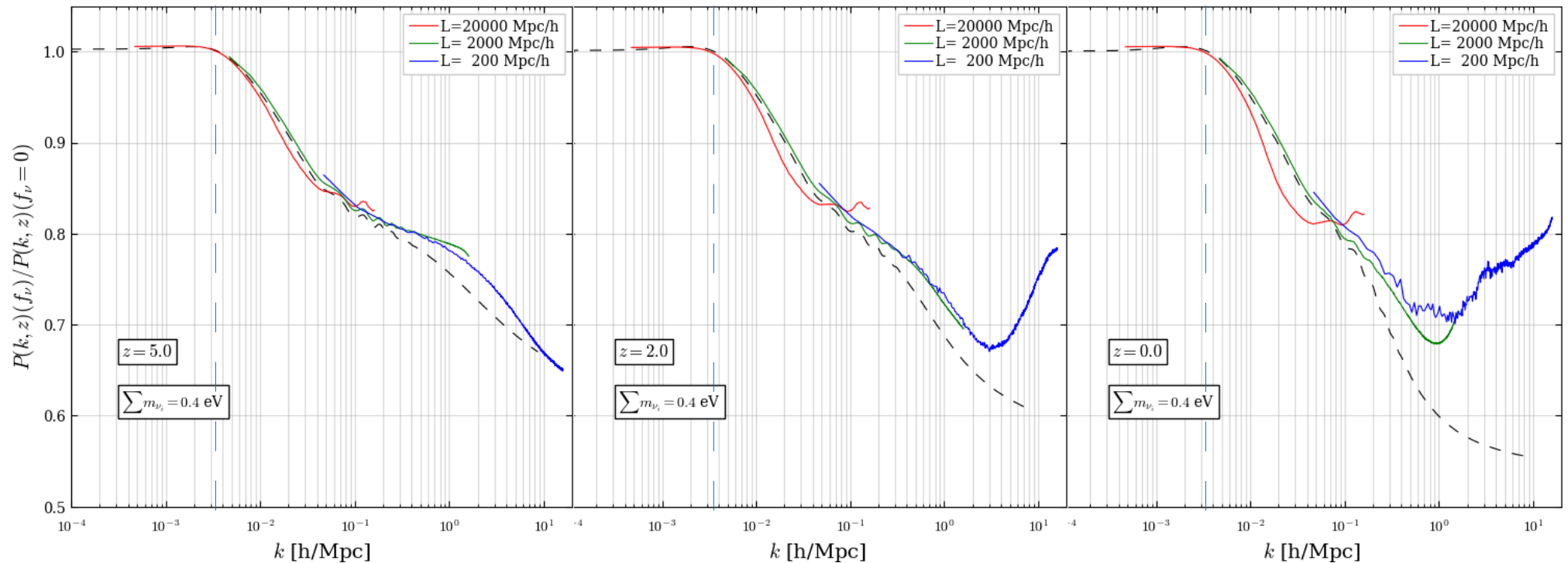
$200 h^{-1} \text{ Mpc}$



$200 h^{-1} \text{ Mpc}$

Power Spectrum

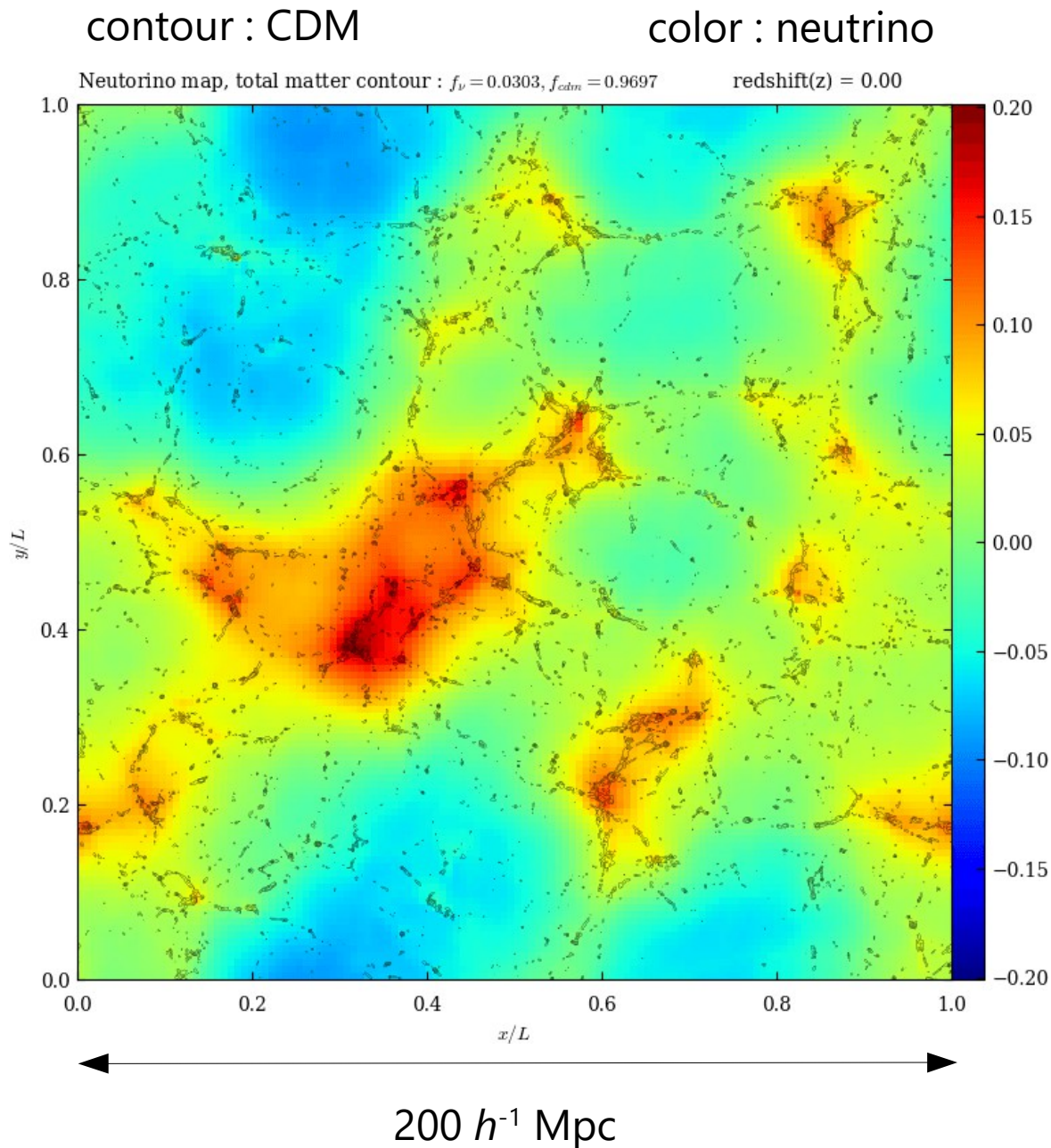
$\frac{P(k, f_\nu)}{P(k, f_\nu = 0)}$: ratio of power spectra with massive and massless neutrinos



damping scale : $k_{\text{nr}} = \sqrt{\frac{4\pi G \bar{\rho}(t_{\text{nr}}) a(t_{\text{nr}})^2}{\sigma_\nu^2(t_{\text{nr}})}} \simeq 0.018 \Omega_{\text{m}}^{1/2} \left(\frac{m}{1 \text{ eV}} \right)^{1/2} h \text{ Mpc}^{-1} = 3.5 \times 10^{-3} h \text{ Mpc}^{-1}$

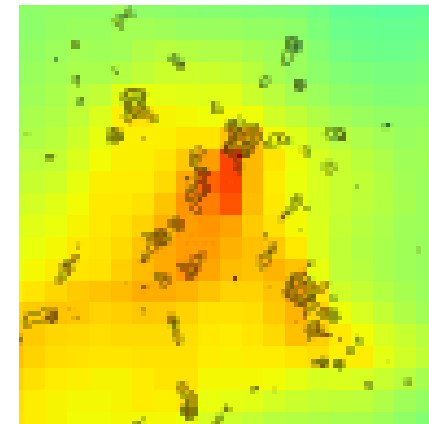
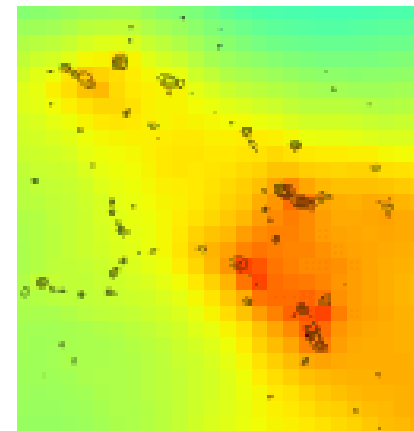
- density fluctuation with $k > 3 \times 10^{-2} h/\text{Mpc}$ damps owing to collisionless damping
- consistent with the perturbation theory (e.g. Saito et al. 2009) in the early stages
- up turn at $k > 1 h^{-1} \text{Mpc}$, probably due to dynamical feedback by CDM

CDM and neutrino distribution



- ▶ diffuse distribution of neutrinos owing to its large velocity dispersion
- ▶ regions with similar CDM density can have significantly different neutrino density
- ▶ remarkable offset in density peaks of CDM and neutrinos
neutrino wake / dynamical friction ?

Zhu et al. (2016)



Vlasov-Maxwell Simulation

Vlasov-Maxwell Simulation

$$\frac{\partial f_s}{\partial t} + \mathbf{v} \cdot \frac{\partial f_s}{\partial \mathbf{x}} + \frac{q_s}{m_s} \left(\mathbf{E} + \frac{\mathbf{v} \times \mathbf{B}}{c} \right) \cdot \frac{\partial f_s}{\partial \mathbf{v}} = 0$$

$$\frac{\partial \mathbf{E}}{\partial t} = c \nabla \times \mathbf{B} - 4\pi \mathbf{J}$$

$$\mathbf{J} = \sum_s \int q_s \mathbf{v} f_s d^3 v$$

$$\frac{\partial \mathbf{B}}{\partial t} = -c \nabla \times \mathbf{E}$$

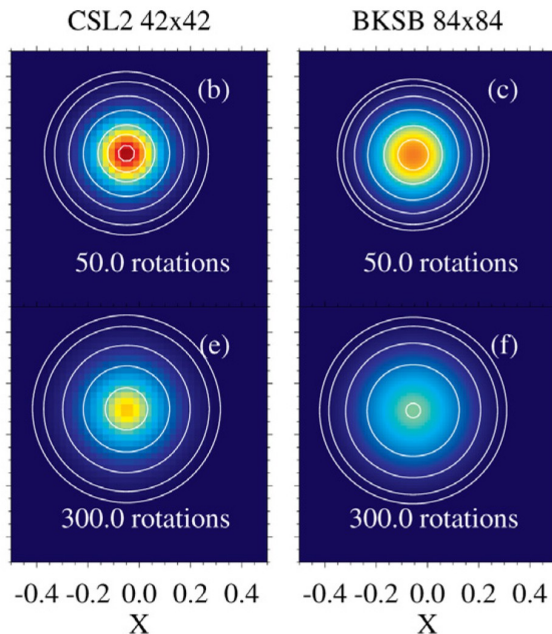
► solve the distribution functions for both of ions and electrons

► difficulty to solve gyro-motion in the velocity space correctly in a long term

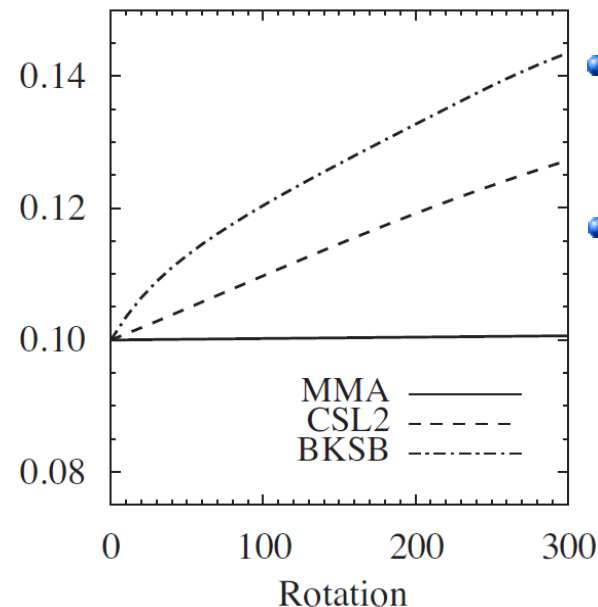
► rigid-body rotation problem

$$\frac{\partial f}{\partial t} + (\mathbf{r} \times \boldsymbol{\omega}) \cdot \frac{\partial f}{\partial \mathbf{r}} = 0$$

rigid-body rotation of a 2D gaussian profile



temporal variation of dispersion



• CSL2 : **CIP-CSL2**

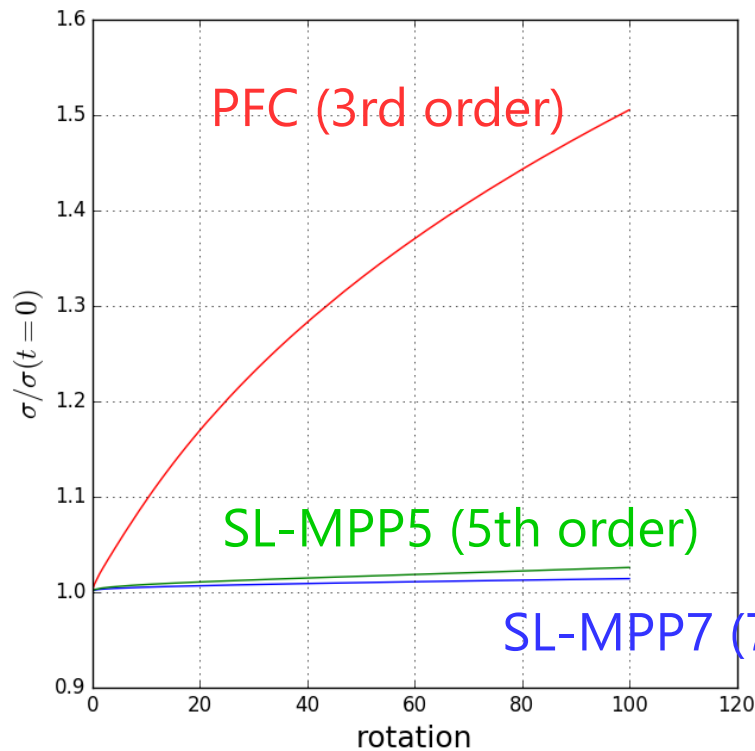
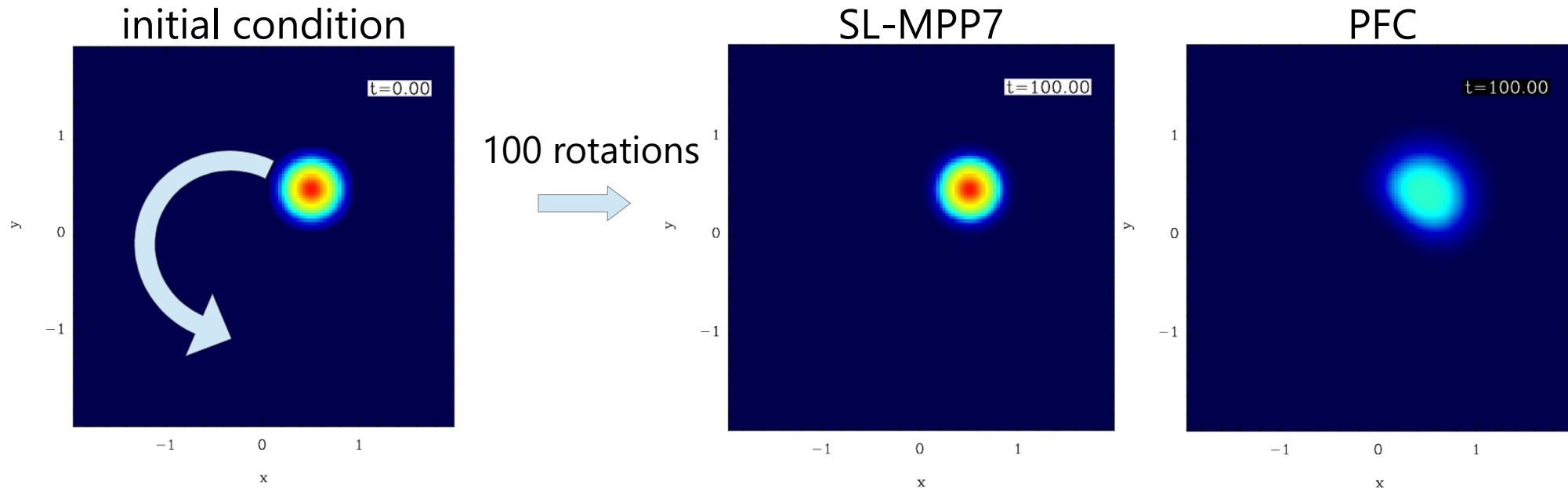
Takizawa et al. (2002)

• BKSB :

backsubstitution method

Schmitz & Grauer (2006)

Rigid-Body Rotation with Our Scheme



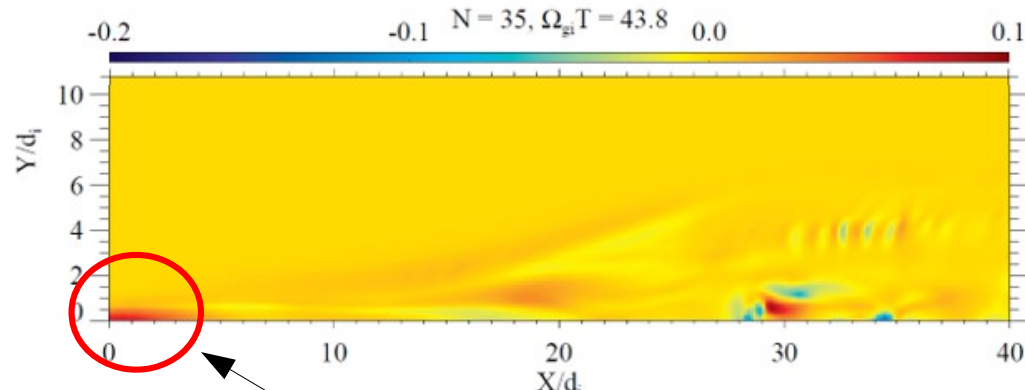
- rigid-body rotation of a gaussian profile in a 2D plane
- SL-MPP5 and SL-MPP7 schemes yields only a few per cent increase in velocity dispersion.
- The lower-order scheme suffers from significant numerical heating.

Magnetic Reconnection with Vlasov-Maxwell Simulations

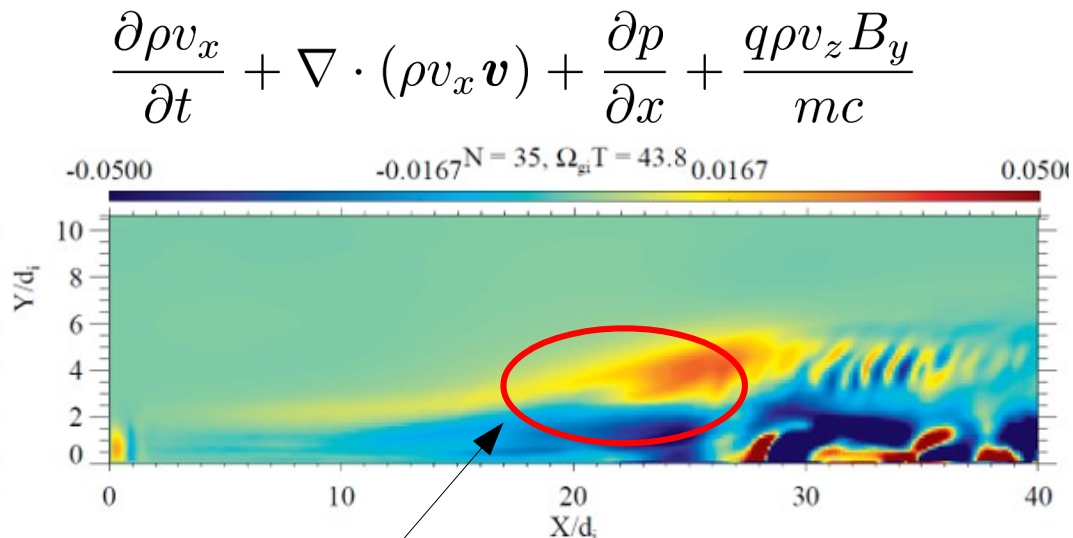
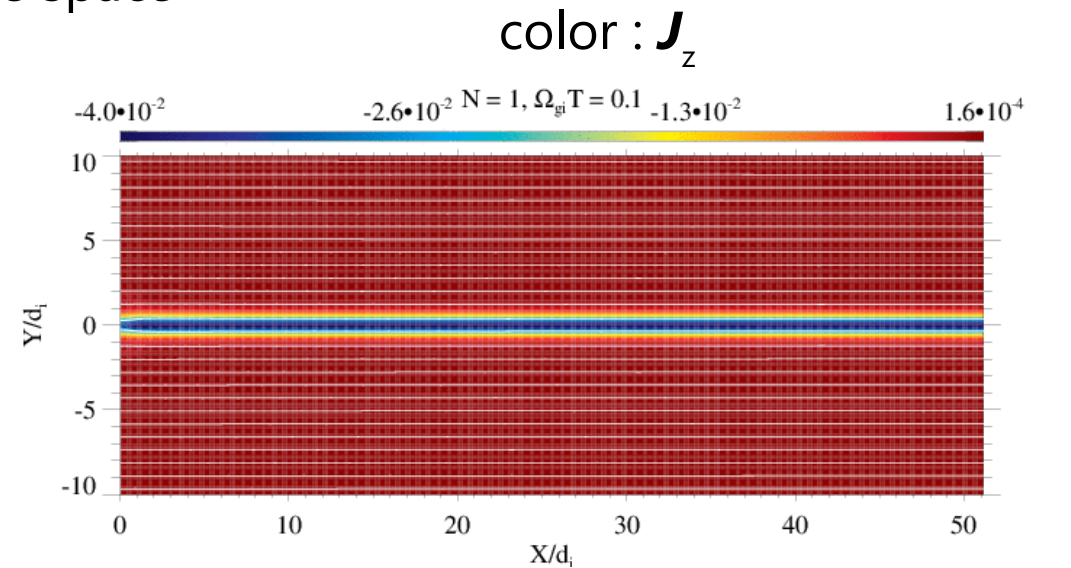
► Vlasov-Maxwell simulation in 5D phase space

- $N_x = 432, N_y = 216$
- $N_{vx} = N_{vy} = N_{vz} = 32$
- Hall effect to trigger the fast reconnection

$$\mathbf{J} \cdot \left(\mathbf{E} + \frac{\mathbf{v} \times \mathbf{B}}{c} \right)$$



dissipation of magnetic field



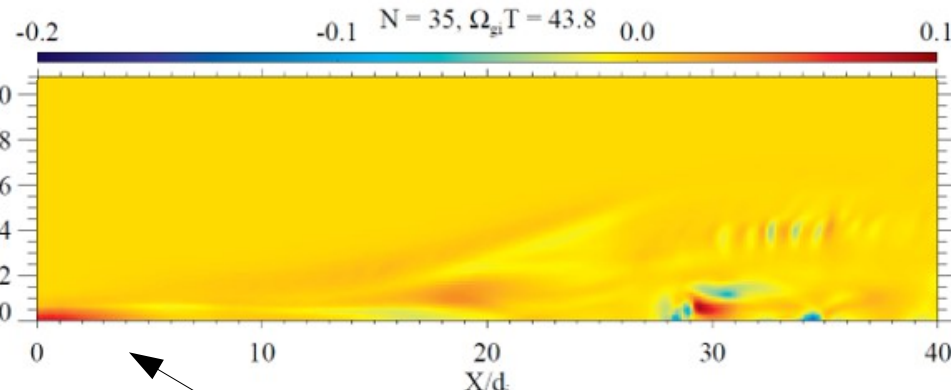
momentum transport to upstream region

Magnetic Reconnection with Vlasov-Maxwell Simulations

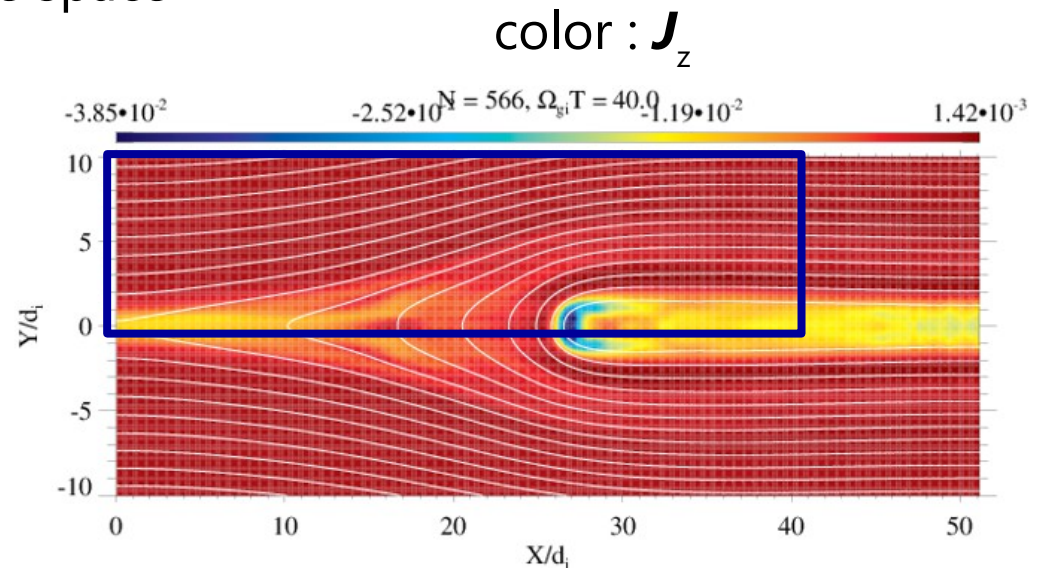
► Vlasov-Maxwell simulation in 5D phase space

- $N_x = 432, N_y = 216$
- $N_{vx} = N_{vy} = N_{vz} = 32$
- Hall effect to trigger the fast reconnection
- Deviation from MHD approximation

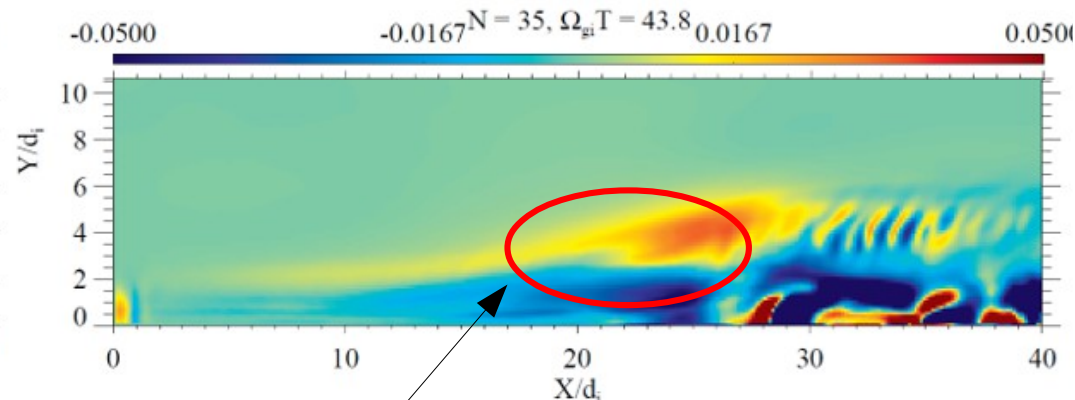
$$\mathbf{J} \cdot \left(\mathbf{E} + \frac{\mathbf{v} \times \mathbf{B}}{c} \right)$$



dissipation of magnetic field



$$\frac{\partial \rho v_x}{\partial t} + \nabla \cdot (\rho v_x \mathbf{v}) + \frac{\partial p}{\partial x} + \frac{q \rho v_z B_y}{mc}$$



momentum transport to upstream region

Summary

- ▶ Vlasov simulations in 6-dimensional phase space are now practical.
- ▶ New high-order advection schemes with monotonicity- and positivity-preservation and with single-stage time integration
- ▶ Vlasov-Poisson simulation of cosmic neutrinos in the large-scale structure in the universe
- ▶ Our new schemes are also suitable for Vlasov-Maxwell simulation owing to good accuracy in rigid-body rotation.
- ▶ Vlasov-Maxwell simulations of magnetic reconnection in 5D phase space show kinetic features of magnetic reconnection in a macroscopic MHD scale.